Structure dependence of molecular reactions on surfaces

Cao, K.

Chapter 6

The two faces of step defects in O_2 reaction on Pt

6.1 Introduction

Molecular oxygen's dissociation on the surface of platinum - a metal typically used as catalyst in proton exchange membrane (PEM) fuel cells [3] and to treat automotive exhaust gases [2]- is known to be complex [114, 115]. Besides a physisorbed state, in which the molecule shows rotational and vibrational characteristics very similar to gas phase O_2 [116–119], there are at least two molecular chemisorbed states. A superoxo species, O_2^-, and a peroxo species, O_2^{2-}, have been identified on the large atomically flat planes of a Pt(111) single crystal [119–122]. These molecular states are precursors to dissociation, which leaves two adsorbed oxygen atoms, O_{ads}, on the surface. The dynamics of adsorption show parallel characteristics of direct and precursor-mediated processes, although the latter contributes only significantly at low surface temperatures [123, 124]. Dissociation does not happen directly upon impact, but proceeds via molecular chemisorbed states [125, 126].

Although easiest to model from a theoretical perspective, Pt(111) is not very representative of the surface structure dominating nanometer-sized Pt catalyst particles. Experimental molecular dynamics studies on various nanostructured Pt surfaces [109, 127, 128] show that step edges induce a dominance of the indirect dissociation mechanism - one presumably proceeding via the physisorbed molecular state [123]. Scanning Tunneling Microscopy (STM) and Temperuture Programmed

Desorption (TPD) studies confirm that monoatomic steps are more reactive in dissociating O_2 than (111) terraces [129, 130]. Theoretical studies discriminate between various molecularly chemisorbed states, both at steps and terraces [129, 131, 132], but calculations of sticking supporting dynamical multiple processes have so far only considered Pt(111) [133, 134]. A tight-binding molecular dynamics approach also challenged the interpretation of indirect adsorption via a physisorbed state [133].

Recently, two new experimental techniques have been developed that allow detailed testing of surface structure and stereodynamical dependencies in O_2 sticking to surfaces. In combination with supersonic molecular beam techniques, curved single crystal surfaces, were recently shown to resolve outstanding issues regarding the dynamics of Pt catalyzed H_2 dissociation [101]. In combination with a high pressure reactor, step-induced induction of CO oxidation on Pd was revealed [135]. The essential ingredient is the controlled continuous variation of step densities over two orders of magnitude on the surface of a single crystal. The top section of figure 6.2 schematically illustrates such a curved single crystal.

The second new technique is state-selection of O_2 using a magnetic hexapole with subsequent steering of the molecule's rotational axis prior to its impact onto the surface [136, 137]. For Pt(111), this technique provided direct evidence that activated adsorption into the chemisorbed superoxo and peroxo states is sensitive to the orientation of O_2's internuclear axis upon impact [138]. Molecules oriented parallel to the (111) plane more easily find their way into molecular chemisorbed states than those oriented perpendicular to that plane. This phenomenon was also shown to control CO oxidation kinetics [139].

Here, we report on the first experimental study of dynamical dependences combining the above-mentioned new techniques. First, we studied the structure and energy-dependencies for O_2 sticking using a curved Pt single crystal in Leiden, the Netherlands. Subsequently, we studied the orientational dependence for O_2 sticking onto three flat single crystals representing the outer edges and center of the curved crystal in Tsukuba, Japan.

6.2 Experimental methods

For measurements performed in Leiden, the Netherlands, we used the same supersonic molecular beam apparatus as described in our previous study of O_2 sticking and dissociation on Pt(553) [109]. Supersonic expansion of O_2 in various seed gases allows us to vary the incident energy, which we determine by standard time-of-flight (TOF) techniques. Sticking is measured using the King and Wells approach. To attain high local resolution, the molecular beam is skimmed to a rectangular shape with a surface area of 0.12 x 6.0 mm^2 at the curved crystal's position. The curved crystal is cleaned by sputtering at 0.5 keV with $\sim 2.0\ \mu A$ Ar^+ current ($p_{Ar} = 6.0 \times 10^{-6}$ mbar) for 5 minutes at surface temperature, T_s, of 900 K. This is followed by oxidation at the same surface temperature (3 minutes, $p_{O_2} = 3.5 \times 10^{-8}$ mbar) and annealing at 1200 K for 3 minutes. This cleaning procedure is repeated 3-5 times before the last cleaning cycle. For the last cycle, we only sputter and anneal at 850 K. We use LEED and Auger Electron Spetroscopy (AES) (OCI BDL800IR-MCP) to verify surface order and cleanliness across the curved surface.

Two 10 mm diameter flat single crystals exposing either the (533) or (553) surface were used to determine the absolute sticking probabilities for comparison to data obtained with the curved Pt single crystal. These crystals were cleaned by sputtering at 0.5 keV with $\sim 2.0\ \mu A$ Ar^+ current ($p_{Ar} = 6.0 \times 10^{-6}$ mbar) for 5 minutes at surface temperature, T_s, of 900 K. This is followed by oxidation at the same surface temperature (3 minutes, $p_{O_2} = 3.5 \times 10^{-8}$ mbar) and annealing at 1200 K for 3 minutes. This cleaning procedure is repeated 3-5 times before the KW measurement. For flat crystals, we use small hole with diameter of 1.6 mm as the final aperture. The molecular beam is shaped into a cycle with diameter of 3.2 mm at the crystal position.

Stereodynamically sensitive experiments performed in Tsukuba, Japan, were also performed using an apparatus described before [136, 137]. Briefly, supersonically expanded mixtures of O_2 in He pass through a magnetic hexapole containing a variable number of hexapole elements. The number of elements is chosen to optimize the cleanliness of the (2,2) state resolution for each kinetic energy. Three sets of Helmholtz coils are placed on the outside of the UHV chamber that houses the Pt(553), Pt(533) or Pt(111) crystals upon which the state-selected O_2 molecules impinge. Currents through the Helmholtz coils

are alternated every 2 seconds to switch between two impact geometries for O_2 while sticking is measured using the King and Wells technique. Every experiment using two impact geometries is performed at least twice also using the reversed order in alternating between impact geometries. Initial sticking probabilities are obtained by exptrapolating the best fit of a double exponential functional form to data over a nearly 60 s time frame to t = 0. We use two filters to separately fit results for the two impact geometries. This extrapolation removes various convolutions at the start of the experiment. Reported sticking probabilities are averaged for experiments with the original and reversed orders.

A typical KW experiment where the orientation of the incident rotating molecule is switched between helicoptering (H) and cartwheeling along the z axis (C_z) at an incident kinetic energy of 0.33 eV along the [111] normal of Pt(553) is shown in figure 6.1. The main panel shows as a blue line the time-dependent sticking probability during the entire experiment. The solid black and red lines are two fits to the data using a double exponential form. These fits are applied only for selected times that either H or C_z molecules impinge. The filters also cut out the rise times in the signal after switching. The inset in figure 6.1 shows the filters at the top of the graph for the first 20 s of the experiment for H (black) and C_z (red) in a high/low fashion. When the filter is high, data are used for the fit. When it is low, data are not used for the fit. The fits are shown in the inset as dashed black and red traces.

The two initial sticking probablities following from each experiment for a combination of H, C_z, and C_y, or from R and L, are calculated from the fit parameters using t = 0. We also repeat each experiment with reversal of the switching order of the two chosen orientations. Reported values for ratios in the manuscript are calculated from the averages of both orders, e.g. H vs C_z and C_z vs H.

6.3 Results

At the top of Figure 6.2, we present an illutration of our curved Pt single crystal. It curves 31° along $[11\overline{2}]$ with the apex centered at the (111) plane. The macroscopic curvature is a consequence of a smooth variation in density of monoatomic steps of the A and B-types (insets)

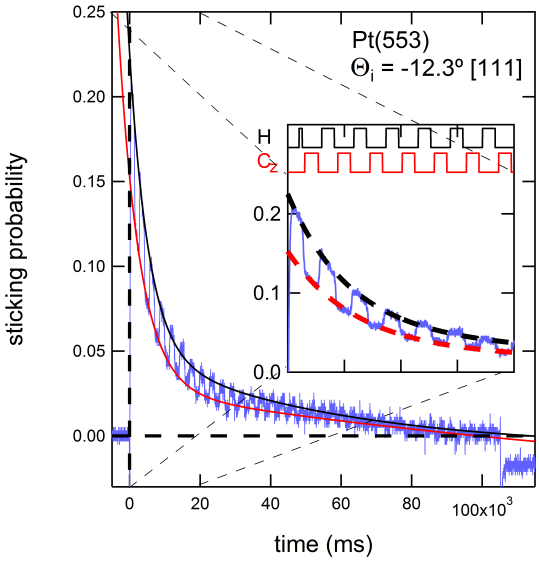

Figure 6.1: An example of a KW measurement for a state-selected (2,2) beam impinging onto Pt(553) at E_{kin} = 0.33 eV and an incident angle of -12.3 ° relative to the surface normal, i.e. along [111]. The Helmholtz coils are set to switch the incident molecules from helicoptering (H) to cartwheeling along the z axis (C_z). The blue line in the main panel shows the KW trace, whereas the black and red solid lines are fits to the data using double exponential functional forms and filters. The inset shows a detail of the KW trace and fits (dashed black and red) for the first 20 s of the experiment. In the upper part of the inset the filters (solid black and red) used to fit the data are shown as high/low for the filter being active/inactive for the indicated rotational orientation of the molecule.

[104, 140]. These A and B-type steps expose, respectively, the shortest possible (100) and (110) facets. We probe the O_2's initial sticking probability, S_0, locally across surface structures from approximately the 6-atom wide (111) planes separated by A-type steps via very large (111) planes at the apex to 6-atom wide (111) planes separated by B-type steps. The width of our molecular beam at the crystal position is 0.12 mm, hence approximately equal to the size of the symbols used to indicate data (open symbols). At the surface temperature of the crystal, T_s, equaling 150 K, the physisorbed state of O_2 is unstable. At the (111) terraces and both steps, O_2 molecules stick molecularly in a chemisorbed state, and/or dissociate. If they (in)directly scatter into the gas phase, it occurs on a time scale much faster than our measurement. The exact final state - dissociated or molecularly chemisorbed - is inconsequential to our findings.

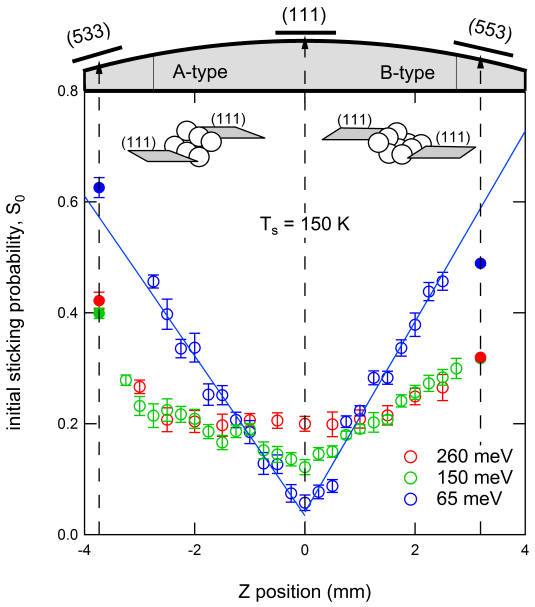

Figure 6.2: Initial sticking probability of O_2 as a function of incident position on a curved Pt single crystal for 65, 150 and 260 meV incident energy at T_s=150 K. Open symbols represent data gathered using the curved single crystal that is schematically represented at the upper side of the graph. Solid symbols were gathered using flat single crystals with (533) and (553) surface structures. Error bars reflect the standard deviation calclulated from multiple measurements. Insets show the local step structure for the A and B type steps.

At the lowest incident energy, E_{kin} = 65 meV, indicated by blue open circles, sticking is linearly dependent on the position over the entire crystal. As the Z position scales linearly with step density, reactivity is a linear sum of independent reactivities at steps and terraces [28, 30]. The solid blue lines represent the best fit to the data at the lowest incident energy. We used only data collected on either the A or B side of the crystal for these fits. Both fits indicate a residual reactivity of 0.04 at the ideal (111) plane. For reference, solid symbols indicate data collected under identical conditions using flat single crystals with (533) and (553) surface structures. These surface structures have 4-atom wide (111) terraces separated by the (100) and (110) facets. Their comparable locations on the curved crystal surface are indicated by vertical dashed lines with arrow heads. Tapering of the polished surface in this regime prohibits accurate measurements using our curved crystal. While for B-types steps, extrapolation of the data

collected on the curved crystal slightly overestimates the reactivity determined for the (553) surface, reactivity is accurately reproduced for the A type step for (533). The steepness of the slopes and their nearly identical absolute values on both sides indicate that the dynamic process resulting in sticking is dominated by steps and insensitive to the local arrangement of Pt atoms forming the step.

At higher incident energies, indicated by the green and red open and solid circles, the reactivity at the (111) apex increases from 0.04 at 65 meV to 0.2 for E_{kin} = 260 meV. The additional contribution of steps diminishes. Reactivity on both sides of the crystal, as well as on the flat (533) and (553) surfaces drops quite dramatically. This energy dependence agrees with previous studies for the (111)[123, 124], (533) [128] and (553)[109] surfaces. Whereas at an incident energy of 150 meV (green), both sides of the crystal still reflect an approximate linear dependence over a reasonably large step density range, at 260 meV the dependence clearly looses it linear character. Beyond 2 mm from the apex, additional kinetic energy has no effect on reactivity, as also found previously for flat single crystals. Particularly A-type steps show non-linear dependence of reactivity on step density in the regime of 4 to 6 atom wide terraces. For wide (111) terraces at the highest incident energy, i.e. near the apex, both step types do not increase reactivity. Clearly, dynamical processes leading to sticking at higher incident energies are not dominated by steps alone.

Figure 6.3 shows the results of experiments testing the dependence of S_0 on the alignment of the O_2 molecule upon impact over a wide range of kinetic energies. A magnetic hexapole selects molecules from a supersonic expansion in the (J,M) = (2,2) state. This state is well described as the $^3\Sigma$ electronic ground with the angular momentum vector of body rotation being aligned parallel to the quantization axis[137]. Coupling of the magnetic moment of this quantum state to an externally applied magnetic field allows us to steer the rotational axis of the molecule prior to impact. In panel a) of figure 6.3, we reproduce with blue diamonds our results published recently for Pt(111)[138]. It plots the ratio of the initial sticking probabilities of molecules impinging onto the surface with a helicoptering motion, $S_0(H)$, and a carthweeling motion, $S_0(C)$, relative to the plane of the Pt surface. As there is no difference for carwheeling motion with respect to the two independent vectors defining the surface plane, we show $S_0(H)/S_0(C)$ without specifying the direction of J with respect to the surface for

cartwheeling molecules. The data clearly show the preference in sticking for helicoptering molecules. This is most explicitly observed at the lowest impact energies, i.e. when the molecule has barely enough kinetic energy to overcome the energetic barrier to chemisorption into a molecular states. This result reflects that chemisorbed states have their O_2 internuclear axis aligned parallel to the surface.

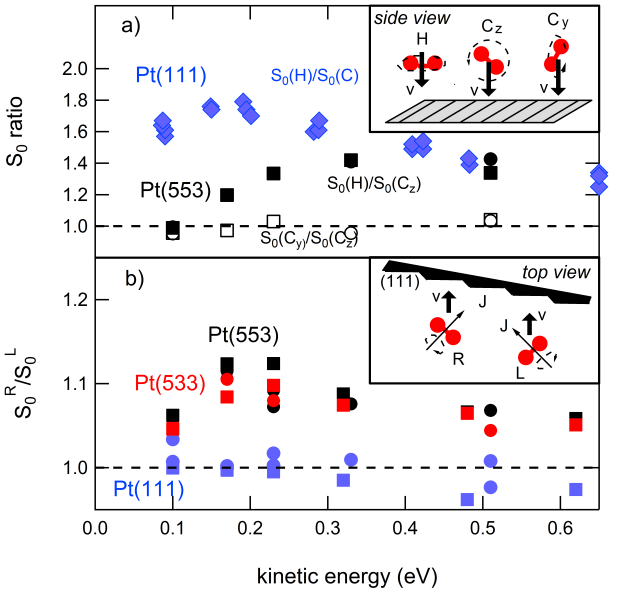

Figure 6.3: In panel a), the sticking probability ratio for helicoptering (H) and cartwheeling (C) O_2 molecules on Pt(111) is shown (blue diamonds) as a function of incident energy. Also shown are the same ratio's for H and C_z (black solid) and C_y and C_z (black open) for Pt(553). Circles indicate impingement along [553], squares along [111]. The inset depicts the various rotational motions relative to the (stepped) surface. Panel b) shows the ratio S_0^R/S_0^L for Pt(111) (blue symbols), Pt(553) (black symbols) and Pt(533) (red symbols) as a function of kinetic energy. The inset depicts the variation in impact geometry for R and L orientations relative to the stepped surfaces. The surface temperature for all data shown in this figure lies in the range of 300 to 400 K.

The black symbols in panel a) of figure 6.3 represent new data, i.e. initial sticking probability ratios for O_2 on Pt(553). Here, we separately show $S_0(H)/S_0(C_z)$ (solid) and $S_0(C_y)/S_0(C_z)$ (open). Circles and squares, which often overlap, differentiate between the experiment being performed with impact along the macroscopic surface normal and impacting along the normal of (111) terraces. The angular difference of $\sim 12°$ has no effect on the results. We separately show the

ratio for C_y and C_z because cartwheeling rotational motion may be sensitive to the alignment of the O_2 axis with respect to the direction of the monoatomic steps on the surface. Data suggest it is rather insensitive to this variation. On the contrary, the ratio of sticking for helicoptering and cartwheeling molecules for Pt(553) clearly deviates from unity. The effects depends on incident energy. While at the lowest kinetic energy the ratio $S_0(H)/S_0(C_z)$ is close to unity, it increases with incident energy to a value of ~ 1.4. This contrasts with the results for Pt(111), where at low energy a strong alignment effect was observed. The B-type steps remove the preference for sticking with a molecular axis parallel to the surface entirely at low incident energy. Notably, at higher incident energy, the sticking probability ratio $S_0(H)/S_0(C_z)$ for the (553) and (111) surfaces merge to the same value.

In panel b) of figure 6.3, we show the results of a different type of experiment. Instead of switching between H and C, we arranged the magnetic field such that molecules flip their rotational axis from +45° (R) to -45° (L) with respect to the velocity vector, v. We ensure that molecules impinge normal to the (111) terraces of three flat single crystals, i.e. Pt(111) (blue), Pt(553) (black) and Pt(533) (red). For the Pt(111) crystal, switching between these R and L states has no effect. These two states are geometrically equivalent on a flat (111) surface. For each energy, we checked that the ratio S_0^R/S_0^L was indeed (nearly) unity for the Pt(111) surface. For the stepped surfaces, this is clearly not the case. Molecules with the J vector oriented as in R, rotate such that the internuclear axis is always roughly parallel to the step facet. To the facet, the molecule looks like it is helicoptering. Rotation as in L combines molecular impact with the internuclear axis being both parallel and orthogonal to the step facet, strongly resembling a cartwheeling motion. Results for A and B type steps, as represented by the Pt(533) and Pt(553) surfaces, indicate that both step types clearly favor molecules impacting with their internuclear axis parallel to the step's (100) or (110) facet. As this experiment is very sensitive to local magnetic fields and details of data analysis, figure 6.3b shows two sets of data by squares and circles gathered independently by two of the authors.

6.4 Discussion

The combined low incident energy results from figure 6.2 and figure 6.3a definitively confirm the hypothesized influence of steps on sticking and dissociation of O_2 at low incident energy. Based on a comparison of the energy-dependence for various stepped Pt surfaces, Jacobse et al. proposed that the dominating contribution to reactivity results from an indirect mechanism that mostly depends on step density[109]. Step type was found not to be of importance to the kinetic energy dependence in the low energy regime. Results of sticking on Pt(533), Pt(553) and Pt(111)(2x1) were nearly identical. The linear dependence of reactivity on step density in figure 6.2 confirms that reactivity is dominated by a dynamical mechanism dependent on steps. The slopes being nearly identical also indicates that this mechanism is indifferent to step type. At the same time, the data in figure 6.3a indicate an independence on the orientation of the internuclear axis at this energy as both sticking probability ratios for molecules with different alignement are all approximately unity. Such indifference is characteristic for a dynamical mechanism that proceeds via a physisorbed state[141]. Such states are only weakly bound. As the potential energy surface for such a state has no strong angular corrugation (they resemble the gas-phase species), scattering into the state is not expected to depend critically on the orientation of the internuclear axis during the collision. The strong dependence on alignment for Pt(111) observed at the lowest energy is a consequence of sticking being predominantly direct into a chemisorbed state. These molecular chemisorbed states are aligned on the surface. Adsorption is favored when the O_2 molecular axis is parallel to the surface during collision. Hence, the lost of the alignment dependence for stepped surfaces in the low energy regime indicates that indirect scattering into a physisorbed state causes the high reactivity as compared to the Pt(111) surface.

With increasing kinetic energy, the results presented in figures 6.3a and 6.3b may seem at odds. While the former suggests that (111) and stepped surfaces have an alignment dependence of equal magnitude at the highest incident energy, favoring H over C with a sticking probability ratio of 1.4, the latter indicate that stepped surfaces show a dependence on alignment whereas (111) does not. However, results in figure 6.3a do not discriminate between alignment effects resulting from impinging onto steps and terraces. At higher incident energies,

the dominance of the dynamical mechanism relying on scattering into a physisorbed state has disappeared. Results in figure 6.2 clearly shows this through the loss of reactivity dependence on step density. Hence, at higher incident energy, direct adsorption into molecular chemisorbed states dominates. This occurs both at steps and terraces. In figure 6.3a, the contributions to direct chemisorption at steps and terraces are mixed. Figure 6.3b, however, shows that the step facets have a unique stereodynamical preference for direct molecular chemisorption as the experimental design removes the contribution of the (111) terraces.

The absolute value of S_0^R / S_0^L seems small in comparison to S_0(H) / S_0(C). It ranges between 1.05 and 1.13, whereas the latter reaches 1.8 for Pt(111). However, this comparison is not fair. The ratio S_0^R / S_0^L results from a minority of O_2 molecules impacting directly onto step sites. Most molecules impact onto the 4-atom wide (111) terraces of the stepped surfaces. The facet may be estimated to contribute at most on the order of one third to the surface area of the unit cell for (533) and (553) [28, 29]. Second, for a quantitative comparison, probability distribution functions for impact with the internuclear axis parallel or perpendicular to any facet need to be taken into account. For the comparison of H and C on (111), the difference in these distributions is largest as H lies truly parallel to the (111) plane. In the R versus L experiment, the facets do not probe the difference as cleanly as their angle from (111) is not 45°. These two considerations suggest that the preference for helicoptering over cartwheeling motion to stick to the step's facet is probably similar to that observed for H and C on Pt(111).

6.5 Concluding remarks

The results of our study show that the influence of steps to alignment dependences in sticking op O_2 are two-faced. Through strongly enhancing the scattering probabilities into a physisorbed state, alignment sensitivity to adsorption and dissociation is entirely lost on highly corrugated surfaces. However, with increasing impact energy, direct adsorption into chemisorbed states becomes increasingly dominant. Similar to (111) terraces, step facets show a preference for molecules being aligned parallel to their surface. Cartwheeling motion relative to the

step direction reduces sticking. The effect shows a clear energy dependence between 0.1 and 0.3 eV, suggesting that adsorption into a chemisorbed state at the step is still (weakly) activated.